

1 **Comprehensive evaluation of AT(N) imaging biomarkers for** 2 **predicting cognition**

3 Tom Earnest¹, Braden Yang¹, Deydeep Kothapalli¹, Aristeidis Sotiras^{1,2}, for the
4 Alzheimer's Disease Neuroimaging Initiative*

5 ¹ Mallinckrodt Institute of Radiology, Washington University School of Medicine in St Louis; 4525 Scott
6 Ave, Saint Louis, MO 63110

7 ² Institute for Informatics, Data Science & Biostatistics, Washington University School of Medicine in St
8 Louis; 660 S. Euclid Ave, Campus Box 8132, Saint Louis, MO 63110

9 * Data used in preparation of this article were obtained from the Alzheimer's Disease Neuroimaging
10 Initiative (ADNI) database (adni.loni.usc.edu). As such, the investigators within the ADNI contributed to
11 the design and implementation of ADNI and/or provided data but did not participate in analysis or writing
12 of this report. A complete listing of ADNI investigators can be found at: [http://adni.loni.usc.edu/wp-](http://adni.loni.usc.edu/wp-content/uploads/how_to_apply/ADNI_Acknowledgement_List.pdf)
13 [content/uploads/how_to_apply/ADNI_Acknowledgement_List.pdf](http://adni.loni.usc.edu/wp-content/uploads/how_to_apply/ADNI_Acknowledgement_List.pdf)

14 Abstract

15 **Background and Objectives:** Imaging biomarkers enable *in vivo* quantification of
16 amyloid, tau, and neurogenerative pathologies that develop in Alzheimer's Disease
17 (AD). Interest in imaging biomarkers has led to a wide variety of biomarker definitions,
18 some of which potentially offer less predictive value than others. We aimed to assess
19 how different operationalizations of AD imaging biomarkers affect prediction of
20 cognition.

21 **Methods:** We included individuals from ADNI who underwent amyloid-PET ($[^{18}\text{F}]$ -
22 Florbetapir), tau-PET ($[^{18}\text{F}]$ -Flortaucipir), and volumetric MRI imaging. We compiled a
23 large collection of imaging biomarker definitions (42 in total) spanning different
24 pathologies (amyloid, tau, neurodegeneration) and variable types (continuous, binary,
25 non-binary categorical). Using cross-validation, we trained regression models to predict
26 neuropsychological performance, both globally and across different subdomains
27 (Phenotype Harmonization Consortium composites), using different combinations of
28 biomarkers. We also compared these biomarker models to support vector machines
29 (SVMs) trained to predict cognition directly from imaging regions of interest. In a
30 subsample of individuals with CSF biomarker readouts, we repeated experiments
31 comparing the accuracy of models using imaging and fluid biomarkers. Additional
32 analyses tested the predictive strength of imaging biomarkers when limited to specific
33 clinical stages of disease (cognitive unimpaired vs. impaired) and when modeling
34 longitudinal cognitive change.

35 **Results:** Our sample included 490 people (247 female) with a mix of no impairment
36 ($n=288$), mild impairment ($n=163$), and dementia ($n=39$). While almost all biomarkers
37 tested were predictive of cognitive performance, we observed substantial variability in
38 accuracy, even for measures of the same pathology. Tau biomarkers were the single
39 most accurate single predictors, though combination of biomarkers spanning multiple
40 pathologies were more accurate overall. SVM models were generally more accurate
41 than models using traditional biomarkers. Incorporating continuous or non-binary
42 categorical biomarkers was beneficial only for tau and neurodegeneration, but not
43 amyloid. Patterns of results were largely consistent when considering different clinical

44 stages of disease, neuropsychological domains, and longitudinal cognition. In the CSF
45 subsample (n=246), imaging biomarkers strongly outperformed CSF versions for
46 cognitive prediction.

47 **Discussion:** We demonstrated that different imaging biomarker definitions can lead to
48 variability in downstream predictive tasks. Researchers should consider how their
49 biomarker operationalizations may help or hinder the assessment of disease severity.

50 Introduction

51 The modern biological definition of Alzheimer's Disease (AD) relies on
52 biomarkers.¹⁻³ Biomarkers can accurately quantify pathobiological disease processes
53 which are specific to AD, particularly the aggregation of amyloid-beta ($A\beta$) plaques and
54 the neocortical spread of tau neurofibrillary tangles. Importantly, biomarkers can detect
55 and measure these pathologies prior to symptomatic onset. Because of their
56 capabilities, biomarkers have been used in a variety of research settings including
57 disease classification⁴, cognitive forecasting⁵, subtype identification⁶, clinical trial
58 stratification⁷, disease staging^{8,9}, and more. Moreover, biomarkers are becoming
59 increasingly important for clinical management of AD². For instance, recently approved
60 anti- $A\beta$ treatments for AD require the presence of $A\beta$ -pathology as assessed by
61 biomarkers.

62 Interest in biological AD assessment has led to the creation of many AD-sensitive
63 biomarkers which vary in terms of modality, underlying pathology, and statistical
64 formulation. Idiosyncrasies of biomarker definitions may result in unwanted variability
65 when applied for clinical and research uses. For example, estimated cut points for PET
66 and CSF biomarker dichotomization are fairly application specific¹⁰⁻¹², and different
67 approaches to pathological thresholding result in considerable variability for group
68 assignment¹³⁻¹⁶. Less is known, however, about how variability in biomarker definitions
69 affects prediction of cognition in AD. Identifying which specific biomarkers are most
70 predictive of cognitive trajectories, particularly at different stages of disease, can provide
71 insight into biological mechanisms of AD. Moreover, precise cognitive decline
72 predictions are valuable for identifying candidates for early therapeutic interventions and
73 for establishing meaningful cognitive endpoints in clinical trials. Despite these
74 implications, investigations into the ramifications of different biomarker
75 operationalizations remain limited. One previous study found that different biomarker
76 definitions varied in their ability to predict longitudinal Mini-Mental State Examination
77 (MMSE) scores, and that dichotomization hindered predictive power of some
78 biomarkers relative to continuous values.¹³ Similar analyses in separate cohorts with
79 additional cognitive measures are needed to confirm and extend these findings,

80 particularly to establish optimal biomarker combinations for both prognostic accuracy
81 and mechanistic insight.

82 Here, we developed a comprehensive set of neuroimaging measures (42 in total)
83 covering the AD core biomarkers A β (A) and tau (T), as well as non-specific biomarkers
84 of neurodegeneration ((N)). We systematically evaluated how different categories of
85 biomarkers and individual variants differ in their ability to predict different cognitive
86 outcomes. While we focused on cross-sectional cognition, we also extended analyses
87 to measures of prospective longitudinal cognition and neuropsychological domains. We
88 additionally incorporated machine learning to test how traditional biomarker approaches
89 compare to methods which can detect more complex, multivariate patterns in imaging
90 data. Finally, we tested multiple CSF biomarkers (20 definitions spanning 4 analytes)
91 and compared their performance with imaging alternatives.

92 **Methods**

93 **Participants**

94 We selected a baseline, cross-sectional sample of Alzheimer's Disease
95 Neuroimaging Initiative (ADNI) participants with tau-PET, A β -PET, and structural MRI
96 imaging data. Exclusion criteria were gaps between scans of greater than 1 year or
97 missing values for any of the following variables: age, sex, *APOE* genotype, Clinical
98 Dementia Rating[®] (CDR) status¹⁷, Phenotype Harmonization Consortium (PHC)
99 cognitive composite scores¹⁸.

100 **Standard protocol approvals, registrations, and patient consents**

101 All participants provided informed written consent for participating in ADNI.
102 Study protocols were approved by site-specific institutional review and ethical boards.

103 **Image acquisition and processing**

104 Detailed descriptions of imaging protocols are provided on the ADNI website¹⁹.
105 Briefly, T1-weighted MRI acquisitions were collected on 3T scanners using an

106 accelerated MPRAGE sequence. A β -PET scans were acquired 50-70 minutes (4
107 frames \times 5 minutes) after a 370 MBq (\pm 10%) injection of [18 F]-Florbetapir. Tau-PET
108 scans were acquired 75-105 minutes (6 frames \times 5 minutes) after a 370 MBq (\pm 10%)
109 injection of [18 F]-Flortaucipir.

110 We accessed processed MRI and PET derivatives generated by the ADNI PET
111 Core. A Freesurfer (v7.1.1) processing pipeline was applied to MRI scans to generate
112 gray matter volumes within regions of interest (ROIs) of standard subcortical²⁰ and
113 cortical atlases²¹. PET standardized uptake value ratios (SUVRs) were generated for
114 these same ROIs after coregistration of each PET image to a contemporaneous MRI
115 scan. Our analyses incorporated unilateral values from 68 cortical and 14 subcortical
116 gray matter regions. Volumes were standardized relative to the intracranial volume.
117 A β -PET uptakes were standardized to a whole cerebellum ROI, while tau-PET uptakes
118 were standardized relative to an ROI containing inferior cerebellar gray matter²².

119 Partial volume corrected (PVC) PET uptakes were available for tau (Geometric
120 Transfer Matrix approach^{23,24}) but not for A β . We used uncorrected SUVR values for
121 most experiments, but we repeated some experiments with PVC-corrected tau SUVRs
122 to evaluate the effect of PVC on cognitive prediction accuracy.

123 Cognitive and clinical assessments

124 Cognition was assessed using composite scores developed by the PHC¹⁸. We
125 averaged the memory (PHC_{Memory}), executive functioning (PHC_{EF}), visuospatial
126 (PHC_{Visual}), and language (PHC_{Language}) composites to create one global cognitive
127 composite (PHC_{Global}). Composites are unitless factor loadings, with lower scores
128 corresponding to more impairment.

129 CDR was used as a measure of dementia severity¹⁷. Subjects were assigned to
130 the following groups based on CDR status: cognitively unimpaired (CU, CDR=0) or
131 cognitively impaired (CI, CDR \geq 0.5).

132 Image-based biomarker definitions

133 We implemented a variety of biomarker definitions to use for predicting cognition.
134 A full list of the biomarker definitions tested is provided in eTable 1. Biomarkers were
135 categorized based on pathology (AT(N)) and variable type (binary [BIN], non-binary
136 categorical [CAT], continuous [CON]). Lists of atlas regions used to form composites
137 are provided in eTable2.

138 Continuous variables consisted of scalar MRI (volume) or PET (SUVR) measures
139 in standard composite ROIs. For A β , continuous measures of A β included the average
140 SUVR in a cortical summary region^{25,26} (A β composite) and Centiloid²⁷. Centiloids were
141 provided by ADNI and derived from the A β composite using previously validated
142 equations²⁸. Continuous tau measures included the average uptakes in a meta-
143 temporal (MT) composite region¹¹ and uptakes in ROIs corresponding to progressive
144 Braak stages^{29,30} (Braak I, Braak III/IV, Braak V/VI). Braak II was omitted due to off-
145 target binding issues with flortaucipir^{31,32}. Hippocampal volume and volume of the MT
146 region were included as continuous assessments of neurodegeneration.

147 Binary predictors consisted of dichotomized versions of the continuous predictors
148 listed above. There were three main methods tested for binarizing continuous
149 variables: previously published cutoffs, Z-scoring, and Gaussian mixture modeling
150 (GMM). Previously published cutoffs were included for the A β composite at the
151 following SUVRs: 1.11³³, 1.24³⁴, 1.30¹¹, 1.42¹¹. We also tested Centiloid cutoffs (15, 20,
152 25, 30) based on ranges reported in previous literature^{28,35,36}. Z-scoring and GMMs
153 were included as data-driven approaches for deriving cutoffs. These methods were
154 applied to the A β composite SUVR, MT tau SUVR, MT volume, and hippocampal
155 volume. Z-scores for each variable were computed relative to CU, A β -negative
156 individuals (using an SUVR cutoff of 1.11 applied to the A β composite to determine A β -
157 negativity, as recommended by the ADNI PET Core). Z-scores were dichotomized
158 using cutoffs of 2 and 2.5 standard deviations away from the CU, A β -negative mean
159 value. GMM binarization was implemented by fitting two-component Gaussian mixtures
160 to the distribution of continuous variables. A cutoff point was estimated as the curve

161 intersection between the fitted Gaussians. GMMs were omitted for hippocampal
162 volume, due to a lack of bimodal distribution.

163 Non-binary categorical biomarkers consisted of quartiles, binarization with an
164 indeterminate zone, and staging systems. Quartiles were computed by binning
165 continuous values at the 25th, 50th, and 75th percentiles. Binarization with an
166 intermediate zone (BIZ) was used to model the uncertainty of assigning individuals who
167 display biomarker values near the cutoff threshold². BIZ was implemented with a GMM,
168 where individuals were marked as uncertain if they showed less than 60% probability of
169 being assigned to either Gaussian component.

170 Staging systems were included as non-binary categorical measures which assign
171 disease severity grades based on the spatial extent of A β or tau pathology. For A β , we
172 applied two previously published staging models^{9,37}. For tau, we implemented two
173 versions of Braak staging with different granularities: Braak staging (6) (I, III, IV, V, VI)
174 and Braak staging (3) (I, III/IV, V/VI). Detailed description of the staging procedures for
175 each of these systems is provided in the eMethods.

176 CSF-based biomarkers

177 We identified a subsample of individuals who had CSF immunoassays within 1
178 year of imaging. CSF samples were analyzed with Roche Elecsys kits sensitive to A β ₄₂,
179 A β ₄₀, total-tau (tTau), and tau phosphorylated at threonine 181 (pTau181). CSF
180 processing was administered by the ADNI Biomarker Core at the University of
181 Pennsylvania.

182 CSF concentrations of analytes were grouped into biomarker categories as
183 previously recommended^{14,151} (A β : A β ₄₂, A β ₄₀, A β ₄₂/A β ₄₀, tau: pTau181,
184 neurodegeneration: tTau). Raw concentrations were included as continuous measures.
185 GMMs were used to define binary versions of CSF biomarkers. BIZ and quartiles were
186 used to generate non-binary categorical versions.

187 Statistical analyses

188 We ran a series of cross-validated modeling experiments to assess how different
189 biomarker definitions compared in their ability to model cognition. Complete details of
190 these experiments are provided in the eMethods. Briefly, we used linear regression
191 models to predict PHC_{Global} using single or multiple biomarker definitions. All regression
192 models also included covariates of age, sex, and *APOE* E4 carriership. Models which
193 only included these covariates were included as controls. Models with single
194 biomarkers were used to test (1) if all included biomarker definitions improved cognitive
195 prediction accuracy and (2) which individual definitions were most predictive of cognitive
196 impairment. Next, we developed linear models combining multiple biomarker definitions
197 as predictors of PHC_{Global} . To limit comparisons for these models, biomarkers were
198 grouped based on the underlying pathology (AT(N)) and the variable type (binary, non-
199 binary categorical, continuous), with nested cross-validation used to select the best
200 predicting definition within each group. These models were used to test (3) if
201 combination of biomarkers improved prediction accuracy, and (4) if models
202 incorporating continuous or non-categorical binary biomarkers outperformed models
203 with binary biomarkers. Next, we trained support vector machines (SVM) to predict
204 PHC_{Global} from regional biomarker values to test if (5) multivariate modeling of AD
205 pathology could improve prediction accuracy beyond that of pre-defined biomarker
206 definitions. SVMs were trained with both linear and non-linear kernels with a grid
207 search to select optimal hyperparameters (see eMethods).

208 All cross-validation experiments had 10 outer folds and were repeated 10 times
209 to generate 100 out of sample error estimates for each tested model. Model error was
210 assessed using root mean squared error (RMSE). Boxplots included in the Results
211 show distributions of the 100 out-of-sample RMSE measurements from trained models.
212 To statistically evaluate differences in accuracy for comparisons of interest, we used
213 Nadeau-Bengio t-tests. The Nadeau-Bengio t-test includes a bias correction for the
214 interdependency of out-of-sample error estimates when using repeated, cross-validated
215 designs^{38,39}. All tests were corrected for multiple comparisons with a false discovery
216 rate method⁴⁰. We investigated feature importance by plotting the distribution of

217 selected biomarkers across folds, the magnitude of the coefficients on biomarkers in
218 linear regression models, and the covariance corrected weights for SVM models⁴¹ (see
219 eMethods). Additionally, we visualized the distribution of model-selected SUVR cutoffs
220 for binary A β - and tau-PET biomarkers.

221 Finally, we ran a series of additional cross-validated experiments using
222 alternative features, target variables, or clinical disease states. Specific experiments
223 were as follows: (a) predicting the prospective slope of PHC_{Global} instead of the cross-
224 sectional value, (b) predicting neuropsychological domains instead of PHC_{Global}, (c)
225 using PVC tau data instead of non-PVC, (d) using CSF-based biomarkers instead of
226 imaging-based versions, and (e) using only CU or CI individuals for model selection and
227 out-of-sample evaluation. For (a), we only included individuals who had longitudinal
228 cognitive measurements following baseline. To estimate longitudinal change in
229 PHC_{Global}, linear mixed effect models were fit to model longitudinal scores following the
230 baseline assessment. Models were fit with random slopes and intercepts for
231 participants.

232 Data availability

233 Data used in the preparation of this article were obtained from the Alzheimer's
234 Disease Neuroimaging Initiative (ADNI) database (adni.loni.usc.edu). The ADNI was
235 launched in 2003 as a public-private partnership, led by Principal Investigator Michael
236 W. Weiner, MD. The primary goal of ADNI has been to test whether serial MRI, PET,
237 other biological markers, and clinical and neuropsychological assessment can be
238 combined to measure the progression of MCI and early AD. For up-to-date information,
239 see www.adni-info.org. All data used in this study are accessible from ADNI following
240 formal data usage agreements. Data were downloaded on May 10th, 2024. All R
241 (v4.4.0) and Python (v3.10) code for this project will be shared at the following
242 repository: https://github.com/sotiraslab/earnest_ad_biomarker_modeling.

243 Results

244 Sample characteristics

245 We selected 490 individuals with baseline biomarker imaging (Table 1). The
246 cohort consisted of a mix of individuals with no cognitive impairment (CDR=0, n=288),
247 very mild dementia (CDR=0.5, n=163), and mild to severe dementia (CDR>0.5, n=39).
248 We observed significant differences in the distribution of age ($p=0.001$), sex ($p=0.005$),
249 $A\beta$ -burden (Centiloid, $p<0.001$), and PHC_{Global} ($p<0.001$) across dementia status. Mean
250 age and $A\beta$ -burden increased with dementia status, while PHC_{Global} decreased.
251 Relatively more females were observed in the CU group (56.6%) than those with very
252 mild (41.1%) or mild to severe dementia (43.6%). *APOE E4* status was not significantly
253 different across groups ($p=0.200$).

254 We also selected subsamples of individuals who had longitudinal PHC_{Global}
255 assessments following baseline (n=383) and those who had CSF biomarker
256 measurements as well as imaging (n=246). Characteristics of these samples are shown
257 in eTables 4 and 5, respectively.

258 Assessment of modeling performance for biomarkers

259 Relative to a control model which included covariates (RMSE=0.531), almost all
260 tested biomarkers led to a significant improvement in prediction accuracy for modeling
261 cognitive scores (Figure 1). The only exception was hippocampal volume binarized at -
262 2.5 Z-scores (RMSE=0.525 [0.06], $p=0.09$). While these results indicated that most
263 biomarker definitions provided some predictive value, gains in performance were not
264 equal across pathologies and variable types (range in RMSE reduction: 3.4-21.1%).
265 Tau biomarkers led to the largest improvements in accuracy, with 9/10 of the best
266 performing biomarkers being tau-based. Furthermore, SVM models which were trained
267 on regional pathology were more accurate than linear models using single biomarker
268 definitions. The tau SVM was the best performing model overall (RMSE=0.419 [0.05],
269 $p<0.001$), while the $A\beta$ SVM (RMSE=0.472 [0.06], $p<0.001$) and volume SVM
270 (RMSE=0.452 [0.05], $p<0.001$) were the best performing $A\beta$ and neurodegeneration

271 models, respectively. Outside of SVMs, the best performing models for each AT(N)
272 category were the A β SUVR binarized at 1.24 (RMSE=0.492 [0.06], $p < 0.001$),
273 continuous MT tau SUVR (RMSE=0.440 [0.05], $p < 0.001$), and continuous MT volume
274 (RMSE=0.471 [0.05], $p < 0.001$).

275 Combination of biomarkers

276 Our next experiments applied a model selection to identify the best performing
277 biomarker predictors based on AT(N) category and variable type. We observed that all
278 biomarker varieties caused a reduction in error over the covariate-only model (Figure
279 2A; mean RMSEs: Covariates=0.531, $A_{BIN}=0.498$, $A_{CAT}=0.495$, $A_{CON}=0.495$, $T_{BIN}=0.470$,
280 $T_{CAT}=0.443$, $T_{CON}=0.440$, $N_{BIN}=0.495$, $N_{CAT}=0.492$, $N_{CON}=0.471$; all $p < 0.01$). Like our
281 experiments (Figure 1), benefits were largest for tau predictors relative to A β and
282 neurodegeneration.

283 Combination models which included assessments for all AT(N) categories
284 generally outperformed models with only one category included. All combination
285 models were more accurate than the covariate-only model in predicting global cognition
286 (mean RMSEs: $A_{BIN}/T_{BIN}/N_{BIN}=0.446$, $A_{CAT}/T_{CAT}/N_{CAT}=0.428$, $A_{CON}/T_{CON}/N_{CON}=0.415$,
287 $A_{SVM}/T_{SVM}/N_{SVM}=0.405$, all $p < 0.001$). Additionally, models which combined biomarkers
288 resulted in significantly higher accuracy than models which only included one pathology
289 assessment (Figure 2A). The benefit of combination was evident for binary
290 ($A_{BIN}/T_{BIN}/N_{BIN}$ vs. A_{BIN} : $t=3.96$, $p < 0.001$; vs. T_{BIN} : $t=2.61$, $p < 0.05$; vs. N_{BIN} : $t=3.92$,
291 $p < 0.001$), non-binary categorical ($A_{CAT}/T_{CAT}/N_{CAT}$ vs. A_{CAT} : $t=4.46$, $p < 0.001$; vs. T_{CAT} :
292 $t=2.22$, $p < 0.05$; vs. N_{CAT} : $t=4.31$, $p < 0.001$), and continuous ($A_{CON}/T_{CON}/N_{CON}$ vs. A_{CON} :
293 $t=5.22$, $p < 0.001$; vs. T_{CON} : $t=3.34$, $p < 0.01$; vs. N_{CON} : $t=4.48$, $p < 0.001$) biomarkers. The
294 combination SVM outperformed the A β ($t=5.29$, $p < 0.001$) and gray matter ($t=3.62$,
295 $p < 0.001$) SVMs, but not the tau SVM ($t=1.56$, $p=0.12$), indicating that the improved
296 accuracy of the multimodal SVM may be primarily driven by tau.

297 Direct comparison of biomarkers based on variable types indicated that
298 biomarker binarization reduced the accuracy for tau and neurodegeneration predictors,
299 but not A β (Figure 2B). Relative to the model with all binary predictors (mean RMSE for

300 $A_{BIN}/T_{BIN}/N_{BIN}=0.446$), reductions in error were seen when incorporating non-binary
301 categorical tau ($A_{BIN}/T_{CAT}/N_{BIN}$: RMSE=0.426, $t=2.14$, $p<0.05$), continuous tau
302 ($A_{BIN}/T_{CON}/N_{BIN}$: RMSE=0.424, $t=2.42$, $p<0.05$), or continuous neurodegeneration
303 ($A_{BIN}/T_{BIN}/N_{CON}$: RMSE=0.432, $t=2.10$, $p<0.05$) biomarkers. An improvement was also
304 observed when including all continuous biomarkers ($A_{CON}/T_{CON}/N_{CON}$: RMSE=0.415,
305 $t=2.99$, $p<0.05$), but not when including all non-binary biomarkers ($A_{CAT}/T_{CAT}/N_{CAT}$:
306 RMSE=0.428, $t=1.56$, $p=0.10$). The tau SVM (RMSE=0.419, $t=2.02$, $p<0.05$) and the
307 AT(N) SVM model (RMSE=0.405, $t=3.42$, $p<0.01$) also outperformed the all-binary
308 model. Models which replaced the binary $A\beta$ definition with a non-binary categorical
309 ($A_{CAT}/T_{BIN}/N_{BIN}$: RMSE=0.446, $t=0.26$, $p=0.60$) or continuous ($A_{CON}/T_{BIN}/N_{BIN}$:
310 RMSE=0.447, $t=0.24$, $p=0.71$) version did not improve accuracy. Improvements were
311 also not seen for $A\beta$ and neurodegeneration SVMs ($p>0.05$).

312 We found no differences in accuracy between models which used PVC for tau
313 SUVRs and ones with no correction (eFigure 1, all $p>0.05$).

314 Feature importance and model interpretation

315 For models which applied nested cross-validation to group biomarkers based on
316 AT(N) category and variable type, the best performing predictors were highly consistent
317 across folds, suggesting that some biomarker definitions generally outperformed others
318 measuring the same pathology (Figure 3A). This was particularly true for tau and
319 neurodegeneration models, where the same biomarker definitions were selected in
320 more than 95% of folds. There was slightly more variation for $A\beta$, but the best
321 performing biomarker was still chosen at least 67% of the time. For PET binarization,
322 previously published cutoffs accounted for 100% of selected $A\beta$ biomarkers, but only
323 1% of tau biomarkers (the other 99% being a GMM applied to the MTT SUVR). For
324 non-binary categorical measures of PET, staging systems appeared to generally
325 outperform other approaches, appearing in 76% of selected $A\beta$ models and 100% of tau
326 models.

327 Inspection of model coefficients highlighted the relative importance of tau for
328 predicting cognition. For linear models which included multiple biomarkers as

329 predictors, coefficients were highest for tau, followed by neurodegeneration and A β
330 (Figure 3B). When considering continuous biomarkers in particular, weights for A β were
331 much lower than those of tau or neurodegeneration. Similarly, the weights for tau
332 features were on average higher than those of A β or atrophy in the multimodal SVM
333 model (Figure 3C). Cortical weights for tau and neurodegeneration highlighted medial
334 and lateral temporal structures, while A β weights were more homogenous. Subcortical
335 regions were weighted lower than cortical ones, except for tau uptake and gray matter
336 volume in the amygdala and hippocampus. Similar spatial patterns were observed
337 when considering the SVM weights from separate A β , tau, and neurodegeneration
338 models (eFigure 2).

339 We used our cross-validated modeling to identify the optimal cutoffs for A β and
340 tau binarization in our cognitive modeling experiments. Our results indicated SUVR
341 cutoffs of 1.26 (range: 1.24-1.30) for A β and 1.44 (range: 1.33-1.45) for tau (Figure 4).

342 Cognitive modeling in CU and CI populations

343 We also trained separate models to optimize the prediction of cognitive scores
344 for individuals who were CU (CDR=0) and those who were CI (CDR>0). Like our
345 results in the whole sample, we found that almost all biomarker models tested resulted
346 in a significant improvement in accuracy relative to a baseline model with just covariates
347 (eFigure 3). These benefits were observed for both CU (range in RMSE reduction: 3.9-
348 15.1%) and CI (range in RMSE reduction: 7.2-30.2%) settings. The only exception was
349 for categorical neurodegeneration models in those CU, where the difference was non-
350 significant ($t=1.65$, $p=0.05$). The best performing models in the CU and CI populations
351 were the all-continuous ($A_{CON}/T_{CON}/N_{CON}$: RMSE=0.349, $t=6.1$, $p<0.001$) and AT(N)
352 SVM models ($A_{SVM}/T_{SVM}/N_{SVM}$: RMSE=0.452, $t=7.5$, $p<0.001$), respectively.

353 Similarly to the whole-sample results, non-binary measures of tau and
354 neurodegeneration, but not A β , provided additional accuracy for modeling PHC_{Global} in
355 CU and CI individuals (eFigure 4). Larger benefits were seen for models including non-
356 binary tau and neurodegeneration in CI individuals relative to CU individuals. For CU
357 individuals (mean RMSE for $A_{BIN}/T_{BIN}/N_{BIN}$: 0.381), we observed improvements when

358 including non-binary categorical tau ($A_{\text{BIN}}/T_{\text{CAT}}/N_{\text{BIN}}$: RMSE=0.366, $t=2.8$, $p<0.05$),
359 continuous tau ($A_{\text{BIN}}/T_{\text{CON}}/N_{\text{BIN}}$: RMSE=0.366, $t=2.6$, $p<0.05$), or continuous biomarkers
360 ($A_{\text{CON}}/T_{\text{CON}}/N_{\text{CON}}$: RMSE=0.359, $t=2.5$, $p<0.05$). Considering CI people (mean RMSE
361 for $A_{\text{BIN}}/T_{\text{BIN}}/N_{\text{BIN}}$: 0.523), we observed increases in accuracy for the categorical tau
362 ($A_{\text{BIN}}/T_{\text{CAT}}/N_{\text{BIN}}$: RMSE=0.490, $t=2.6$, $p<0.05$), continuous tau ($A_{\text{BIN}}/T_{\text{CON}}/N_{\text{BIN}}$:
363 RMSE=0.485, $t=3.3$, $p<0.01$), continuous neurodegeneration ($A_{\text{BIN}}/T_{\text{BIN}}/N_{\text{CON}}$:
364 RMSE=0.495, $t=3.4$, $p<0.01$), continuous AT(N) ($A_{\text{CON}}/T_{\text{CON}}/N_{\text{CON}}$: RMSE=0.479, $t=3.4$,
365 $p<0.01$), tau SVM (T_{SVM} : RMSE=0.484, $t=2.4$, $p<0.05$), and AT(N) SVM
366 ($A_{\text{SVM}}/T_{\text{SVM}}/N_{\text{SVM}}$: RMSE=0.442, $t=4.8$, $p<0.001$) models.

367 Modeling longitudinal cognition

368 The pattern of results we observed were largely consistent when modeling
369 prospective change in cognition. All model varieties tested were significantly more
370 accurate for predicting longitudinal change in $\text{PHC}_{\text{Global}}$ (range in RMSE reduction: 4.1-
371 30.3%, all $p<0.05$) relative to a covariate-only model (eFigure 5a), with the largest
372 benefits seen for the all-continuous ($A_{\text{CON}}/T_{\text{CON}}/N_{\text{CON}}$: RMSE=0.386, $t=5.83$, $p<0.001$),
373 multimodal SVM ($A_{\text{SVM}}/T_{\text{SVM}}/N_{\text{SVM}}$: RMSE=0.368, $t=5.44$, $p<0.001$), and tau SVM (T_{SVM} :
374 RMSE=0.373, $t=5.44$, $p<0.001$). No biomarker linear models with non-binary measures
375 improved prediction accuracy relative to an all-binary baseline (eFigure 5b, all $p>0.05$).
376 However, the tau SVM (T_{SVM} : RMSE=0.373, $t=3.05$, $p<0.01$) and multimodal SVM
377 ($A_{\text{SVM}}/T_{\text{SVM}}/N_{\text{SVM}}$: RMSE=0.368, $t=3.54$, $p<0.01$) were still significantly more accurate at
378 predicting change in $\text{PHC}_{\text{Global}}$ than a model consisting of all-binary predictors.

379 Modeling of individual neuropsychological domains

380 We also observed similar patterns of accuracy differences for non-binary
381 biomarker definitions when modeling neuropsychological domains instead of $\text{PHC}_{\text{Global}}$.
382 Significant benefits were only observed for models which included non-binary or SVM-
383 based assessments of tau and neurodegenerative pathology (eFigure 6). Models which
384 included non-binary definitions of $A\beta$ alone did not surpass the all-binary model for any
385 neuropsychological domain. Continuous tau and neurodegeneration measures
386 improved accuracy for prediction of PHC_{EF} ($p<0.05$) and $\text{PHC}_{\text{Visual}}$ ($p<0.05$), while non-

387 binary categorical measures only improved prediction of $\text{PHC}_{\text{Visual}}$ ($p < 0.05$). The AT(N)
388 SVM had significantly higher accuracy for modeling PHC_{EF} ($p < 0.01$), $\text{PHC}_{\text{Visual}}$ ($p < 0.05$),
389 and $\text{PHC}_{\text{Memory}}$ ($p < 0.05$). No significant differences were observed for $\text{PHC}_{\text{Language}}$
390 prediction accuracy (all $p > 0.05$).

391 Comparison of image-based and CSF-based models

392 We observed that CSF-based models performed relatively poorly for modeling
393 cognition. Models which incorporated CSF-based biomarkers, as opposed to imaging-
394 based ones, did not perform better than a baseline model consisting of only covariates
395 (Figure 5 & eFigure 7, all $p > 0.05$). Moreover, imaging-based models were significantly
396 more accurate than CSF-based models. This was true for binary ($t = 2.81$, $p < 0.01$), non-
397 binary categorical ($t = 3.68$, $p < 0.01$), and continuous ($t = 3.96$, $p < 0.01$) biomarker
398 definitions.

399 Discussion

400 AD biomarkers differ from each other along various axes such as the underlying
401 pathology they measure (e.g. $A\beta$, tau), the modality (e.g., imaging, CSF, blood), and
402 measurement characteristics (e.g., variable type). Our analyses indicate that
403 differences along these dimensions result in considerable variability when imaging
404 biomarkers are utilized in downstream tasks. We show that even biomarkers which
405 assess the same pathology exhibit a range in accuracy when applied for modeling
406 cognition. Additionally, we demonstrate that multivariate machine learning approaches
407 can surpass traditional biomarker definitions for cognitive prediction in AD. Careful
408 consideration should be applied when selecting biomarker definitions for predictive
409 tasks, as certain operationalizations may be relatively less informative than other
410 variants. While we specifically focus on cognitive prediction, our results may be
411 relevant for other settings where researchers wish to quantify AD pathology.

412 While nearly all tested biomarkers provided predictive gains when modeling
413 cognition, some categories of biomarkers yielded consistently larger improvements than
414 others. Multiple analyses demonstrated that tau biomarkers exhibited stronger

415 associations with cognition than assessments of A β or neurodegeneration, a well-
416 documented finding.^{42–44} Feature importance analyses indicated that tau predictors
417 were weighted higher than A β or neurodegeneration measures in models which
418 incorporated all three AT(N) categories. However, combined AT(N) models generally
419 outperformed unimodal ones, even when tau was the single biomarker included. Thus,
420 while measures of tau are important indicators of cognitive decline, incorporation of
421 measures spanning other pathologies is warranted for enhancing predictive accuracy.

422 We observed that SVM models outperformed more traditional linear models of
423 cognition. Tau and multimodal SVMs were the best predictors overall in many
424 experiments. These models were also the only models which outperformed binary
425 biomarker models for prediction of longitudinal cognitive decline. A β and
426 neurodegeneration SVMs were also relatively stronger than other individual biomarker
427 definitions of these pathologies. The superior performance of SVM models suggest that
428 there may be key predictive signal occurring in brain regions external to the manually
429 defined meta-ROIs which are utilized in most of the biomarker definitions we tested.
430 However, the SVMs also allowed for non-linear transformations of input features,
431 making them relatively more powerful models.

432 Inclusion of non-binary tau and neurodegeneration predictors led to small but
433 consistent improvements in accuracy relative to binary alternatives. However, binary A β
434 measures performed equally to non-binary ones. As such, our findings indicate that
435 binarization along dimensions of tau and neurodegeneration (e.g., labeling individuals
436 as T+/- or N+/-) may obfuscate information relevant to the prediction of cognitive
437 decline. On the other hand, dichotomization of A β status may be sufficient. These
438 notion agrees with revised criteria for diagnosis and staging of AD²: their proposed PET
439 staging system includes binary assessment of A β (i.e., has AD or not) and multi-level
440 staging of tau based on the extent of progression outside the medial temporal lobe.
441 Interestingly, the specific benefits for tau and neurodegeneration (and not A β) were
442 consistent when considering only CU or CI individuals and when modeling some
443 neuropsychological domains (executive functioning and visuospatial performance).
444 These results agree with a previous study which found similar non-dichotomized tau

445 and neurodegeneration for modeling longitudinal cognitive decline¹³. However, we did
446 not replicate their findings showing accuracy improvements when modeling prospective
447 cognition in CU individuals and including non-binary measures of A β .

448 While nearly all the imaging biomarkers we tested improved prediction of
449 cognitive impairment, the same was not true for CSF counterparts. Models which
450 incorporated CSF biomarkers as predictors did not perform better than baseline models
451 which only included standard covariates, regardless of the analyte or its
452 operationalization. Previous findings have similarly demonstrated stronger associations
453 for imaging biomarkers and cognitive scores in AD, relative to fluid biomarkers⁴⁵.
454 Importantly, the CSF analytes tested largely reflect earlier pathological cascades which
455 likely develop and saturate prior to the onset of neurodegeneration and cognitive
456 decline^{2,46}. As such, they may be less suited for providing direct associations with
457 cognitive decline, and more suited for diagnosis or prediction of future decline.

458 Our study has limitations which should be considered. First, while we performed
459 a comprehensive and rigorous evaluation of multiple biomarkers, biomarkers such as
460 fluorodeoxyglucose-PET, cortical thickness, and functional imaging were not included in
461 this study. Future studies are warranted to examine them. Second, this study relied
462 only on ADNI because inclusion of other sources posed issues of harmonization and
463 biomarker availability. While ADNI is one of few databases which can enable the
464 analyses we conducted, it is also relatively limited in its inclusion of demographic
465 diversity⁴⁷. As such, our results warrant replication in other datasets.

466 The growth of large data initiatives has led to an explosion of approaches for
467 biomarker assessment of AD. While picking from the myriads of methods for
468 quantification of AD pathology, it is important for researchers to mind the biological,
469 statistical, and practical characteristics of each approach. Our results demonstrate that
470 different operationalizations of the same pathology can result in variable performance
471 for downstream predictive tasks. More complex indices of pathology may be superior to
472 dichotomous alternatives, particularly for measures of neurodegeneration and tau.
473 Finally, data-driven, machine learning approaches may be preferable for identifying
474 biomarker contributions to cognitive decline.

475 **Acknowledgement**

476 The authors thank the staff for the Washington University Center for High
477 Performance Computing who helped enable this work. Computations were performed
478 using the facilities of the Washington University Research Computing and Informatics
479 Facility (RCIF). The RCIF has received funding from NIH S10 program grants:
480 1S10OD025200-01A1 and 1S10OD030477-01.

481 **Study Funding**

482 This work was supported by the National Institutes of Health (NIH) (R01-
483 AG067103) and the BrightFocus Foundation (ADR A2021042S).

484 Data collection and sharing for this project was funded by the Alzheimer's
485 Disease Neuroimaging Initiative (ADNI) (National Institutes of Health Grant U01
486 AG024904) and DOD ADNI (Department of Defense award number W81XWH-12-2-
487 0012). ADNI is funded by the National Institute on Aging, the National Institute of
488 Biomedical Imaging and Bioengineering, and through generous contributions from the
489 following: AbbVie, Alzheimer's Association; Alzheimer's Drug Discovery Foundation;
490 Araclon Biotech; BioClinica, Inc.; Biogen; Bristol-Myers Squibb Company; CereSpir,
491 Inc.; Cogstate; Eisai Inc.; Elan Pharmaceuticals, Inc.; Eli Lilly and Company;
492 EuroImmun; F. Hoffmann-La Roche Ltd and its affiliated company Genentech, Inc.;
493 Fujirebio; GE Healthcare; IXICO Ltd.; Janssen Alzheimer Immunotherapy Research &
494 Development, LLC.; Johnson & Johnson Pharmaceutical Research & Development
495 LLC.; Lumosity; Lundbeck; Merck & Co., Inc.; Meso Scale Diagnostics, LLC.; NeuroRx
496 Research; Neurotrack Technologies; Novartis Pharmaceuticals Corporation; Pfizer Inc.;
497 Piramal Imaging; Servier; Takeda Pharmaceutical Company; and Transition
498 Therapeutics. The Canadian Institutes of Health Research is providing funds to support
499 ADNI clinical sites in Canada. Private sector contributions are facilitated by the
500 Foundation for the National Institutes of Health (www.fnih.org). The grantee
501 organization is the Northern California Institute for Research and Education, and the
502 study is coordinated by the Alzheimer's Therapeutic Research Institute at the University

503 of Southern California. ADNI data are disseminated by the Laboratory for Neuro
504 Imaging at the University of Southern California.

505 Disclosures

506 Author AS has equity in TheraPanacea and have received personal
507 compensation for serving as grant reviewer for BrightFocus Foundation. The remaining
508 authors have no conflicting interests to report.

509 References

- 510 1. Jack CR, Bennett DA, Blennow K, et al. NIA-AA Research Framework: Toward a
511 biological definition of Alzheimer's disease. *Alzheimer's & Dementia*.
512 2018;14(4):535-562. doi:10.1016/j.jalz.2018.02.018
- 513 2. Jack CR, Andrews JS, Beach TG, et al. Revised criteria for diagnosis and staging of
514 Alzheimer's disease: Alzheimer's Association Workgroup. *Alzheimer's &
515 Dementia*. Published online June 27, 2024:alz.13859. doi:10.1002/alz.13859
- 516 3. Hansson O. Biomarkers for neurodegenerative diseases. *Nat Med*. 2021;27(6):954-
517 963. doi:10.1038/s41591-021-01382-x
- 518 4. Rathore S, Habes M, Iftikhar MA, Shacklett A, Davatzikos C. A review on
519 neuroimaging-based classification studies and associated feature extraction
520 methods for Alzheimer's disease and its prodromal stages. *NeuroImage*.
521 2017;155:530-548. doi:10.1016/j.neuroimage.2017.03.057
- 522 5. McConathy J, Sheline YI. Imaging Biomarkers Associated With Cognitive Decline: A
523 Review. *Biological Psychiatry*. 2015;77(8):685-692.
524 doi:10.1016/j.biopsych.2014.08.024
- 525 6. Chen P, Zhang S, Zhao K, Kang X, Rittman T, Liu Y. Robustly uncovering the
526 heterogeneity of neurodegenerative disease by using data-driven subtyping in
527 neuroimaging: A review. *Brain Research*. 2024;1823:148675.
528 doi:10.1016/j.brainres.2023.148675
- 529 7. Abdelnour C, Agosta F, Bozzali M, et al. Perspectives and challenges in patient
530 stratification in Alzheimer's disease. *Alzheimers Res Ther*. 2022;14:112.
531 doi:10.1186/s13195-022-01055-y
- 532 8. Earnest T, Bani A, Ha SM, et al. Data-driven decomposition and staging of
533 flortaucipir uptake in Alzheimer's disease. *Alzheimer's & Dementia*. 2024;20(6).
534 doi:10.1002/alz.13769

- 535 9. Collij LE, Heeman F, Salvadó G, et al. Multitracer model for staging cortical amyloid
536 deposition using PET imaging. *Neurology*. 2020;95(11):e1538-e1553.
537 doi:10.1212/WNL.0000000000010256
- 538 10. Klunk W, Cohen A, Bi W, et al. Why we need two cutoffs for amyloid imaging: Early
539 versus Alzheimer's-like amyloid-positivity. *Alzheimer's & Dementia*. 2012;8(4,
540 Supplement):P453-P454. doi:10.1016/j.jalz.2012.05.1208
- 541 11. Jack CR, Wiste HJ, Weigand SD, et al. Defining imaging biomarker cut-points for
542 brain aging and Alzheimer's disease. *Alzheimers Dement*. 2017;13(3):205-216.
543 doi:10.1016/j.jalz.2016.08.005
- 544 12. Weigand AJ, Maass A, Eglit GL, Bondi MW. What's the cut-point?: a systematic
545 investigation of tau PET thresholding methods. *Alzheimers Res Ther*. 2022;14(1):49.
546 doi:10.1186/s13195-022-00986-w
- 547 13. Mattsson-Carlgrén N, Leuzy A, Janelidze S, et al. The implications of different
548 approaches to define AT(N) in Alzheimer disease. *Neurology*. 2020;94(21):e2233-
549 e2244. doi:10.1212/WNL.0000000000009485
- 550 14. Salimi Y, Domingo-Fernández D, Hofmann-Apitius M, et al. Data-Driven
551 Thresholding Statistically Biases ATN Profiling across Cohort Datasets. *J Prev*
552 *Alzheimers Dis*. 2024;11(1):185-195. doi:10.14283/jpad.2023.100
- 553 15. Provost K, Iaccarino L, Soleimani-Meigooni DN, et al. Comparing ATN-T designation
554 by tau PET visual reads, tau PET quantification, and CSF PTau181 across three
555 cohorts. *Eur J Nucl Med Mol Imaging*. 2021;48(7):2259-2271. doi:10.1007/s00259-
556 020-05152-8
- 557 16. Bucci M, Chiotis K, Nordberg A. Alzheimer's disease profiled by fluid and imaging
558 markers: tau PET best predicts cognitive decline. *Mol Psychiatry*. 2021;26(10):5888-
559 5898. doi:10.1038/s41380-021-01263-2
- 560 17. Morris JC. Clinical Dementia Rating: A Reliable and Valid Diagnostic and Staging
561 Measure for Dementia of the Alzheimer Type. *International Psychogeriatrics*.
562 1997;9(S1):173-176. doi:10.1017/S1041610297004870
- 563 18. Mukherjee S, Choi SE, Lee ML, et al. Cognitive Domain Harmonization and
564 Cocalibration in Studies of Older Adults. *Neuropsychology*. 2023;37(4):409-423.
565 doi:10.1037/neu0000835
- 566 19. ADNI Study Documents. Alzheimer's Disease Neuroimaging Initiative. 2024.
567 Accessed May 15, 2024. <https://adni.loni.usc.edu/methods/documents/>
- 568 20. Fischl B, Salat DH, Busa E, et al. Whole brain segmentation: automated labeling of
569 neuroanatomical structures in the human brain. *Neuron*. 2002;33(3):341-355.
570 doi:10.1016/s0896-6273(02)00569-x

- 571 21. Desikan RS, Ségonne F, Fischl B, et al. An automated labeling system for
572 subdividing the human cerebral cortex on MRI scans into gyral based regions of
573 interest. *NeuroImage*. 2006;31(3):968-980. doi:10.1016/j.neuroimage.2006.01.021
- 574 22. Diedrichsen J. A spatially unbiased atlas template of the human cerebellum.
575 *Neuroimage*. 2006;33(1):127-138. doi:10.1016/j.neuroimage.2006.05.056
- 576 23. Baker SL, Maass A, Jagust WJ. Considerations and code for partial volume
577 correcting [18F]-AV-1451 tau PET data. *Data in Brief*. 2017;15:648-657.
578 doi:10.1016/j.dib.2017.10.024
- 579 24. Rousset OG, Ma Y, Evans AC. Correction for partial volume effects in PET: principle
580 and validation. *J Nucl Med*. 1998;39(5):904-911.
- 581 25. Mormino EC, Kluth JT, Madison CM, et al. Episodic memory loss is related to
582 hippocampal-mediated beta-amyloid deposition in elderly subjects. *Brain*.
583 2009;132(Pt 5):1310-1323. doi:10.1093/brain/awn320
- 584 26. Jagust WJ, Landau SM, Shaw LM, et al. Relationships between biomarkers in aging
585 and dementia. *Neurology*. 2009;73(15):1193-1199.
586 doi:10.1212/WNL.0b013e3181bc010c
- 587 27. Klunk WE, Koeppe RA, Price JC, et al. The Centiloid Project: standardizing
588 quantitative amyloid plaque estimation by PET. *Alzheimers Dement*. 2015;11(1):1-
589 15.e1-4. doi:10.1016/j.jalz.2014.07.003
- 590 28. Royse SK, Minhas DS, Lopresti BJ, et al. Validation of amyloid PET positivity
591 thresholds in centiloids: a multisite PET study approach. *Alzheimers Res Ther*.
592 2021;13(1):99. doi:10.1186/s13195-021-00836-1
- 593 29. Braak H, Braak E. Neuropathological staging of Alzheimer-related changes. *Acta*
594 *Neuropathol*. 1991;82(4):239-259. doi:10.1007/BF00308809
- 595 30. Braak H, Alafuzoff I, Arzberger T, Kretschmar H, Del Tredici K. Staging of
596 Alzheimer disease-associated neurofibrillary pathology using paraffin sections and
597 immunocytochemistry. *Acta Neuropathol*. 2006;112(4):389-404.
598 doi:10.1007/s00401-006-0127-z
- 599 31. Lemoine L, Leuzy A, Chiotis K, Rodriguez-Vieitez E, Nordberg A. Tau positron
600 emission tomography imaging in tauopathies: The added hurdle of off-target binding.
601 *Alzheimers Dement (Amst)*. 2018;10:232-236. doi:10.1016/j.dadm.2018.01.007
- 602 32. Biel D, Brendel M, Rubinski A, et al. Tau-PET and in vivo Braak-staging as
603 prognostic markers of future cognitive decline in cognitively normal to demented
604 individuals. *Alzheimer's Research & Therapy*. 2021;13(1):137. doi:10.1186/s13195-
605 021-00880-x

- 606 33. Landau SM, Mintun MA, Joshi AD, et al. Amyloid deposition, hypometabolism, and
607 longitudinal cognitive decline. *Annals of Neurology*. 2012;72(4):578-586.
608 doi:10.1002/ana.23650
- 609 34. Su Y, Flores S, Wang G, et al. Comparison of Pittsburgh compound B and
610 florbetapir in cross-sectional and longitudinal studies. *Alzheimers Dement (Amst)*.
611 2019;11:180-190. doi:10.1016/j.dadm.2018.12.008
- 612 35. Salvadó G, Molinuevo JL, Brugulat-Serrat A, et al. Centiloid cut-off values for
613 optimal agreement between PET and CSF core AD biomarkers. *Alzheimer's*
614 *Research & Therapy*. 2019;11(1):27. doi:10.1186/s13195-019-0478-z
- 615 36. Farrell ME, Jiang S, Schultz AP, et al. Defining the Lowest Threshold for Amyloid-
616 PET to Predict Future Cognitive Decline and Amyloid Accumulation. *Neurology*.
617 2021;96(4):e619-e631. doi:10.1212/WNL.00000000000011214
- 618 37. Mattsson N, Palmqvist S, Stomrud E, Vogel J, Hansson O. Staging β -Amyloid
619 Pathology With Amyloid Positron Emission Tomography. *JAMA Neurology*.
620 2019;76(11):1319-1329. doi:10.1001/jamaneurol.2019.2214
- 621 38. Nadeau C, Bengio Y. Inference for the Generalization Error. *Machine Learning*.
622 2003;52(3):239-281. doi:10.1023/A:1024068626366
- 623 39. Bouckaert RR, Frank E. Evaluating the Replicability of Significance Tests for
624 Comparing Learning Algorithms. In: Dai H, Srikant R, Zhang C, eds. *Advances in*
625 *Knowledge Discovery and Data Mining*. Lecture Notes in Computer Science.
626 Springer; 2004:3-12. doi:10.1007/978-3-540-24775-3_3
- 627 40. Benjamini Y, Hochberg Y. Controlling the False Discovery Rate: A Practical and
628 Powerful Approach to Multiple Testing. *Journal of the Royal Statistical Society:*
629 *Series B (Methodological)*. 1995;57(1):289-300. doi:10.1111/j.2517-
630 6161.1995.tb02031.x
- 631 41. Haufe S, Meinecke F, Görgen K, et al. On the interpretation of weight vectors of
632 linear models in multivariate neuroimaging. *NeuroImage*. 2014;87:96-110.
633 doi:10.1016/j.neuroimage.2013.10.067
- 634 42. Gordon BA, McCullough A, Mishra S, et al. Cross-sectional and longitudinal atrophy
635 is preferentially associated with tau rather than amyloid β positron emission
636 tomography pathology. *Alzheimers Dement (Amst)*. 2018;10:245-252.
637 doi:10.1016/j.dadm.2018.02.003
- 638 43. La Joie R, Visani AV, Baker SL, et al. Prospective longitudinal atrophy in
639 Alzheimer's disease correlates with the intensity and topography of baseline tau-
640 PET. *Sci Transl Med*. 2020;12(524):eaau5732. doi:10.1126/scitranslmed.aau5732
- 641 44. Ossenkoppele R, Smith R, Mattsson-Carlgrén N, et al. Accuracy of Tau Positron
642 Emission Tomography as a Prognostic Marker in Preclinical and Prodromal

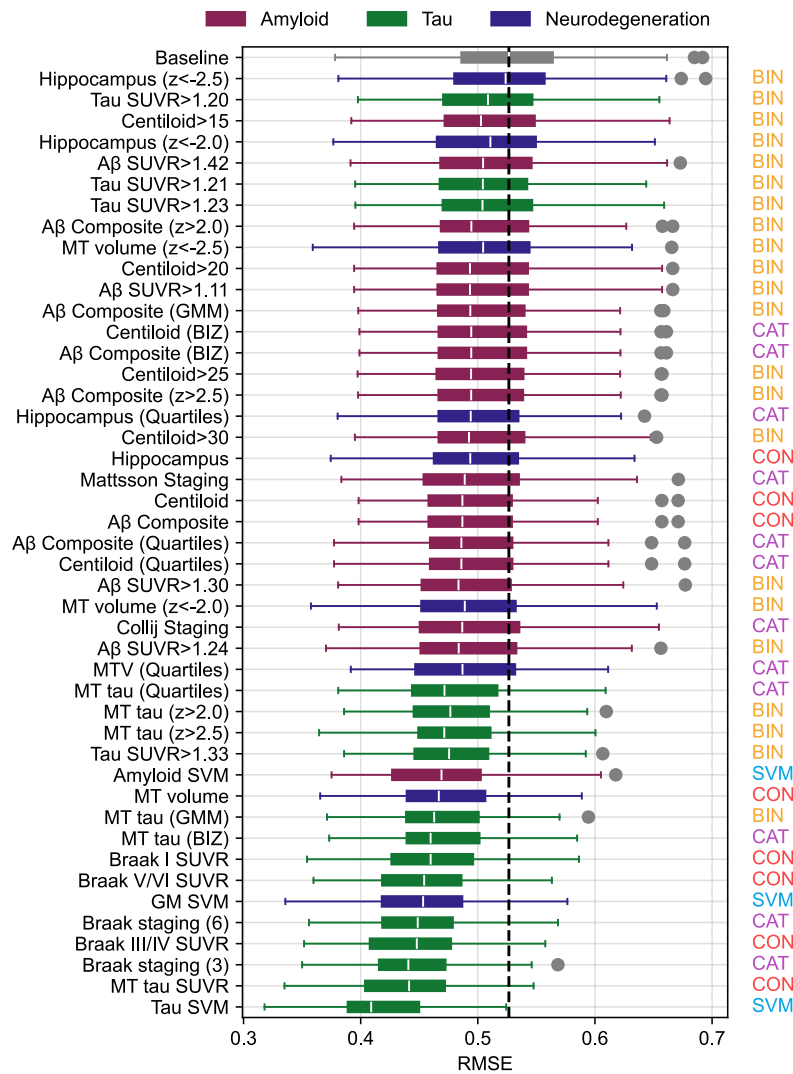
- 643 Alzheimer Disease: A Head-to-Head Comparison Against Amyloid Positron
644 Emission Tomography and Magnetic Resonance Imaging. *JAMA Neurology*.
645 2021;78(8):961-971. doi:10.1001/jamaneurol.2021.1858
- 646 45. Lu J, Ma X, Zhang H, et al. Head-to-head comparison of plasma and PET imaging
647 ATN markers in subjects with cognitive complaints. *Transl Neurodegener*.
648 2023;12(1):34. doi:10.1186/s40035-023-00365-x
- 649 46. Tissot C, Therriault J, Kunach P, et al. Comparing tau status determined via plasma
650 pTau181, pTau231 and [18F]MK6240 tau-PET. *eBioMedicine*. 2022;76:103837.
651 doi:10.1016/j.ebiom.2022.103837
- 652 47. Weiner MW, Veitch DP, Miller MJ, et al. Increasing participant diversity in AD
653 research: Plans for digital screening, blood testing, and a community-engaged
654 approach in the Alzheimer's Disease Neuroimaging Initiative 4. *Alzheimer's &*
655 *Dementia*. 2023;19(1):307-317. doi:10.1002/alz.12797
- 656

657 Tables

	CDR=0.0	CDR=0.5	CDR=1.0+	p-value
n	288	163	39	
Age	73.84 (7.44)	75.78 (8.46)	78.29 (8.58)	0.001
Sex (M/F)	125/163	96/67	22/17	0.005
APOE E4+	99 (34.4%)	62 (38.0%)	19 (48.7%)	0.200
Centiloid	19.90 (36.10)	45.57 (54.95)	78.41 (49.61)	<0.001
PHC_{Global}	0.81 (0.36)	0.32 (0.46)	-0.42 (0.54)	<0.001

658 **Table 1:** Sample characteristics. The last column shows p-values for significance tests
659 comparing distributions of variables across dementia status groups (CDR). Chi-squared
660 tests of association were used for categorical variables (sex, APOE status) and one-
661 way ANOVAs were used for continuous variables (age, Centiloid, PHC_{Global}).

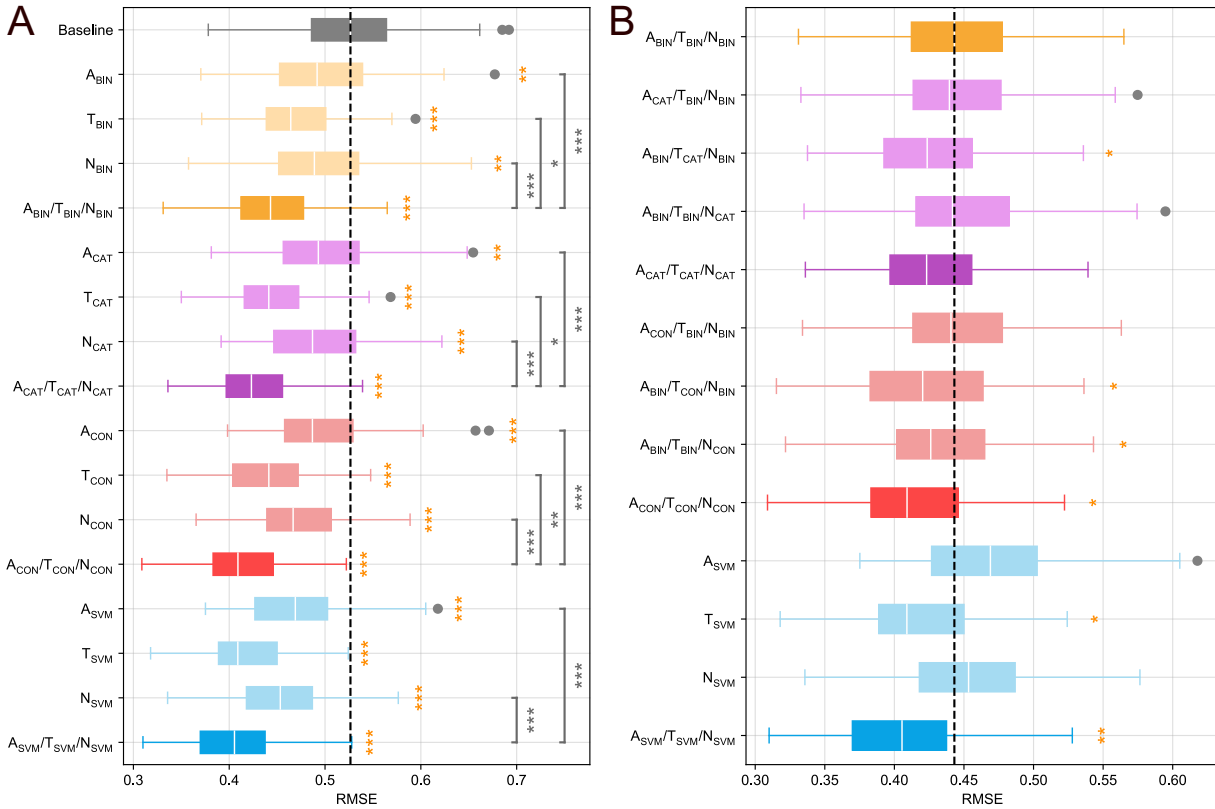
662 Figures



663

664 **Figure 1:** Boxplots showing performance of individual biomarkers for predicting
 665 PHC_{Global}. Values plotted are RMSEs taken from out of sample predictions for 100
 666 cross-validation instances (lower value is more accurate). The baseline model only
 667 included covariates as independent variables (mean performance for this model
 668 indicated by the dotted line). All other models included the same covariates and a
 669 single amyloid (maroon), tau (green), or neurodegeneration (blue) biomarker. Labels on
 670 the right indicate the variable type of each biomarker (BIN=binary, CAT=non-binary
 671 categorical, CON=continuous, SVM=support vector machine). All models exhibited
 672 significantly lower RMSE than the baseline model, except for hippocampal volume
 673 binarized at -2.5 Z-scores [Hippocampus (z<-2.5)].

674



675

676 **Figure 2:** Boxplots showing RMSE performance of combination biomarkers for
677 predicting global neuropsychological performance (PHC_{Global}). **A.** Individual and
678 combination biomarker models are compared against a baseline model using only
679 covariates (mean performance indicated by dotted line) to predict PHC_{Global}. **B.**
680 Combination biomarker models with non-binary variable types are compared against a
681 baseline model with binary biomarker definitions (mean performance indicated by dotted
682 line). In both panels, colors are used to indicate the variable type of included
683 biomarkers (yellow: binary, purple: non-binary categorical, red: continuous, blue: SVM).
684 Lighter coloring indicates models which only have a single pathology assessment, while
685 darker coloring indicates models which have A β , tau, and neurodegeneration
686 biomarkers. Gold stars indicate a significant improvement in accuracy relative to the
687 topmost model. Gray stars and bars highlight significant pairwise differences between
688 individual models. Statistical results are derived from Nadeau-Bengio t-tests with
689 correction for multiple comparisons (*p<0.05, **p<0.01, ***p<0.001).

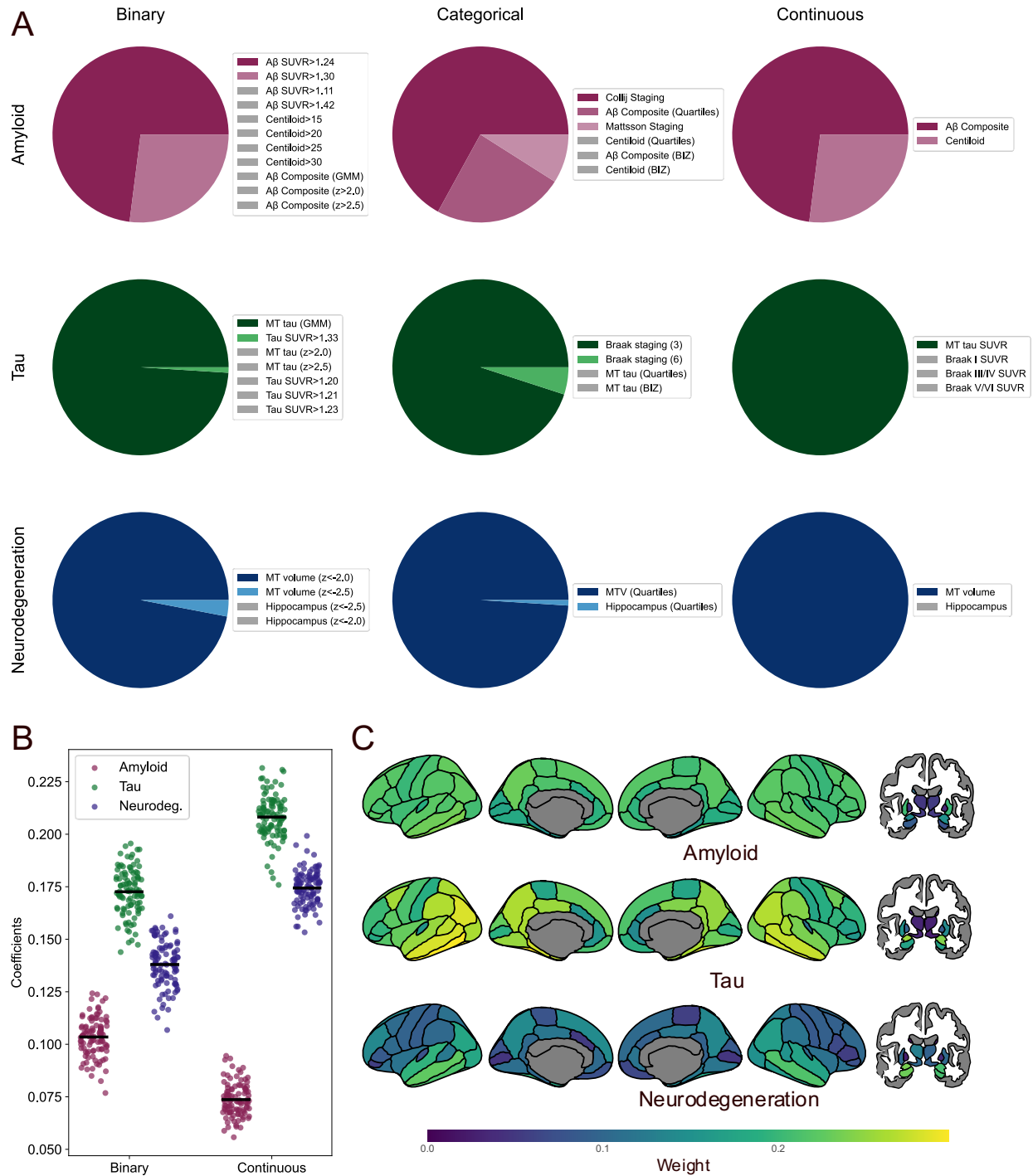
690

691

692

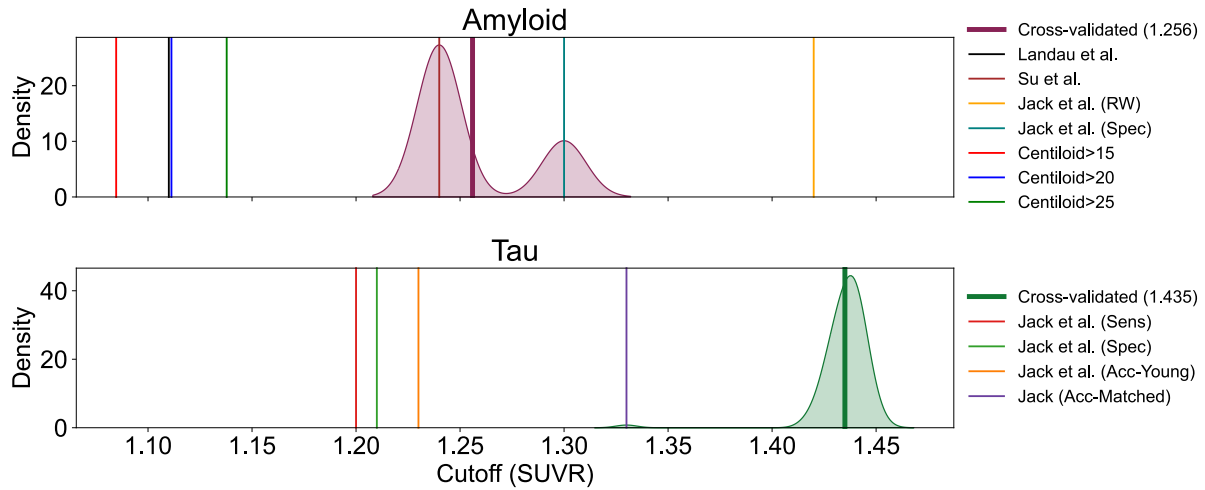
693

It is made available under a [CC-BY-NC 4.0 International license](https://creativecommons.org/licenses/by-nc/4.0/).



694

695 **Figure 3:** Feature importance analysis. **A.** Pie charts showing which biomarkers were selected
 696 as the best performing from cross-validation (100 training fold instances). Biomarkers shown with
 697 gray coloring were not selected in any iteration. **B.** Coefficients for the Aβ, tau, and
 698 neurodegeneration predictor in cross-validated linear models. Values are taken from 100
 699 instances of the all binary ($A_{BIN}/T_{BIN}/N_{BIN}$) and all continuous ($A_{CON}/T_{CON}/N_{CON}$) models. **C.** Brain
 700 maps showing average regional feature importance derived from the $A_{SVM}/T_{SVM}/N_{SVM}$ model.



701

702 **Figure 4.** Estimated cutoffs for A β - and tau-PET binarization. **A.** The kernel density
703 estimation of selected cutoffs for A β (100 cross-validation iterations) is shown in
704 maroon, with the mean value (1.256) highlighted with the bold vertical line. **B.** Same as
705 A., but for tau and shown in green (mean value: 1.435). In both panels, other vertical
706 lines show other pre-defined cutoff values that were tested.

707

708

709

710

711

712

713

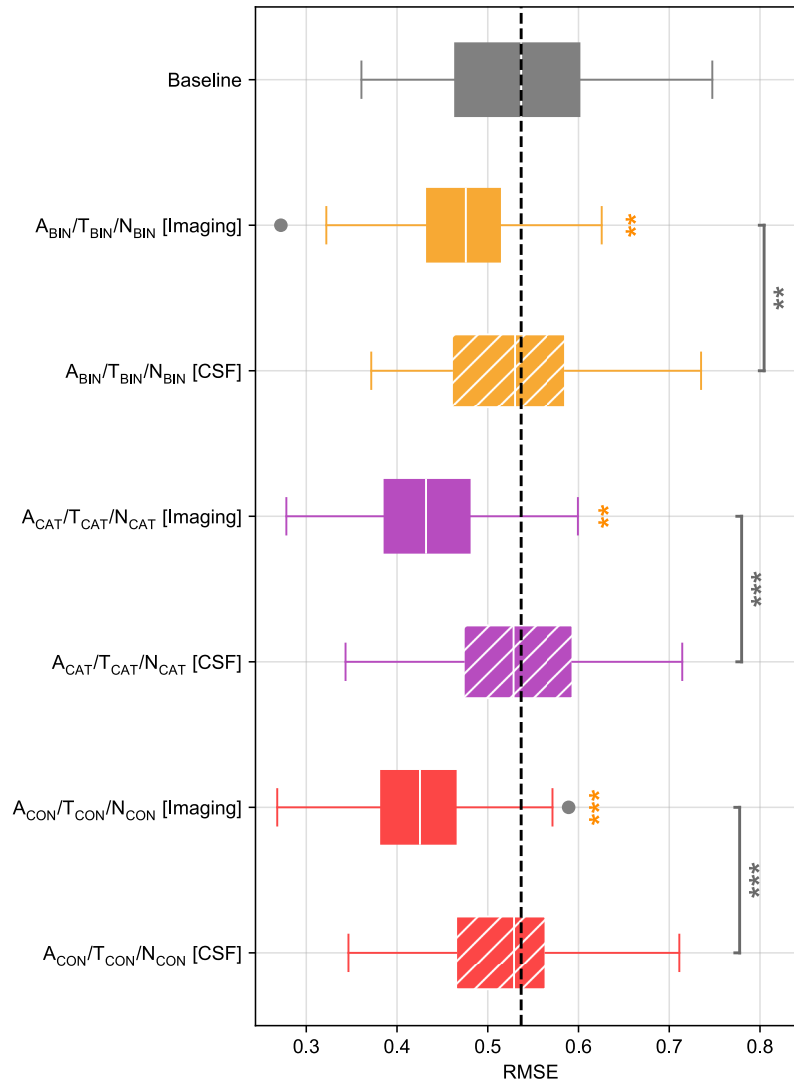
714

715

716

717

718



719

720 **Figure 5.** Boxplots comparing accuracy cognition predictions using image-based (solid)
721 and CSF-based (hatched) biomarkers. Values are RMSEs taken from 100 cross-
722 validation instances. Colors are used to indicated the variable type of included
723 biomarkers (yellow: binary, purple: non-binary categorical, red: continuous). Gold stars
724 indicate a significant improvement in accuracy relative to the baseline model (only
725 covariates). Gray stars and bars highlight significant pairwise differences between
726 individual models. Statistical results are derived from Nadeau-Bengio t-tests with
727 correction for multiple comparisons (* $p < 0.05$, ** $p < 0.01$, *** $p < 0.001$).